NORMAL FAULTING ON EUROPA: IMPLICATIONS FOR ICE SHELL PROPERTIES. F. Nimmo[1] and P. Schenk[2], [1] Dept. Earth Sciences, University of California Santa Cruz, CA 95064 (nimmo@ess.ucla.edu) [2] Lunar and Planetary Institute, Houston, TX 77058 (schenk@lpi.usra.edu).

Introduction: Although Europa's ice shell is pervasively deformed by primarily extensional structures [1], few normal faults have been identified. Here we use stereo topography to characterize two apparent normal faults, and infer both the local Young's modulus and effective elastic thickness for the ice shell.

Observations: Figure 1 shows an area in the trailing hemisphere of Europa. Fig 1a is a context image, and Fig. 1b is a stereo-derived topographic map [2] of the same area. Particularly noteworthy is an elevated plateau with a straight, NNE-trending northern edge and a parallel depression. Fig 1c shows this plateau edge, demonstrating that several features are offset across this edge. We conclude that the edge represents a normal fault, upthrown to the S. Topographic profiles across this plateau support this hypothesis (see Figs. 3 and 4). Figure 2 shows the stereo-derived topography of an area W of Manannan crater. Again, an elevated plateau is evident, with the northern edge of the plateau resembling the topography expected from a normal fault. Images of the same area (not shown) also support this interpretation.

Displacement Profiles: In Figures 3a and 3c the elevation of the uplifted (footwall) and downdropped (hanging-wall) sides of the plateaus are plotted as a function of along-strike distance. The displacement profiles thus obtained (Figs 3b,d) are similar to those of terrestrial normal faults (an example is shown in Fig 3b). The ratios of maximum displacement to fault length (D/L) are ~0.02, comparable to values for faults on silicate bodies [3].

Across-strike Profiles: Figure 4 plots averaged topographic profiles perpendicular to the strike of the inferred faults. In each case, the footwall uplift decays away with a characteristic distance, which on Earth is often used to infer the rigidity, or effective elastic thickness T_e, of the local material [4]. Figures 4a and 4c plot the best-fit theoretical elastic profiles, calculated using the method of [5] and using T_e values of 0.15 km and 1.2 km, respectively. Figures 4b and 4d plot the misfit between observation and theory as a function of T_e, and demonstrate that in each case there is a well-defined minimum.

Mechanical Inferences: Terrestrial D/L ratios have been analyzed using the theory of linear elastic fracture mechanics [6]. While this theory may be an overly simple representation of faulting, it provides a convenient starting point from which to analyze Europan normal faults. Figure 5 plots the expected D/L ratio for normal faults in ice as a function of remote stress and shear modulus μ, using the theory of [6]. The shaded box plots the observed range of D/L ratios. Figure 5 suggests that a) the shear modulus of ice must be much less than its intact value of 4 GPa and b) the remote stresses required are several MPa, much larger than diurnal tidal stresses (<0.1 MPa).

Discussion and Conclusions: The T_e values inferred suggest local conductive shell thicknesses in the range ~1-5 km, and lie between previous T_e estimates [7-9]. Local extension factors are small (<10%) and are unlikely to greatly affect the ice shell thermal structure.

The low inferred shear modulus is consistent with models [10] in which the near-surface ice is highly porous and/or pervasively fractured. Such high near-surface porosity may have important implications for the radar and seismic properties of the ice [11]. Motion on the larger fault will generate an event of seismic magnitude M_s~5.3, considerably larger than the cracking events considered by [11].

The high driving stresses required are much greater than diurnal stresses, and probably exceed the stresses generated by polar wander or non-synchronous rotation. However, they can be easily explained by the stresses which arise from progressive thickening of a floating ice shell [12].

References: [1] Figueredo P.H. and Greeley R. (2004) *Icarus 167*, 287-312. [2] Schenk P.M. (2002) *Nature., 417*, 419-21. [3] Watters T.R. et al. (2000) *Geophys. Res. Lett., 27*, 3659-62. [4] Brown C.D. and Phillips R.J. (1999) *Tectonics, 18*, 1275-91. [5] Kusznir N. J. et al., (1991), *Geol. Soc. Sp. Pub., 56*, 41-60. [6] Cowie, P.A. and Scholz, C.H. (1992). *J. Struct. Geol., 14*, 1149-56. [7] Hurford T.A. et al. (2004). *LPS XXXV*, 1831. [8] Billings, S. E. and S. A. Kattenhorn (2002). *LPS XXXII*, 1813. [9] Nimmo F. et al. (2003). *Geophys. Res. Lett. 30*, 1233. [10] Nimmo F. et al. (2003). Icarus 166, 21-32. [11] Lee S. W. et al. (2003). *Icarus 165*, 144-67. [12] Nimmo F. (2004). *J. Geophys. Res. 109*, E12001. [13] Manighetti I. et al. (2001). *J. Geophys. Res. 106*, 13667-96.

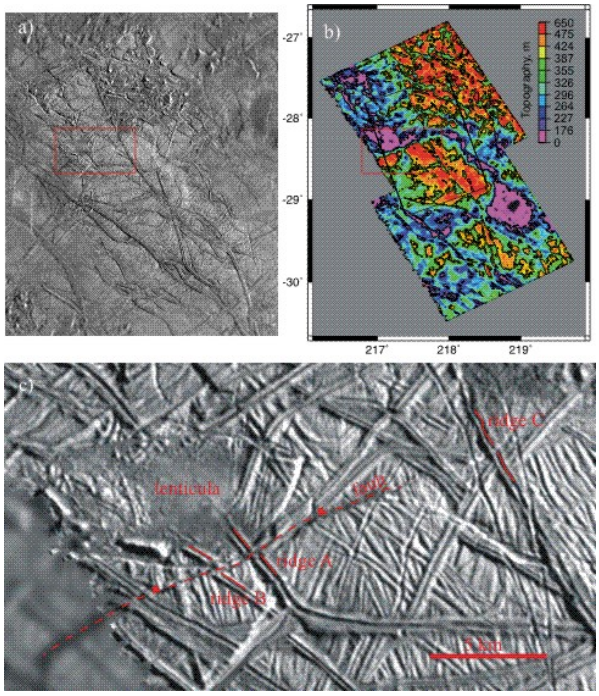

Figure 1. a) Image from Galileo observation sequence 17EDISSTR01, 55m/pix. Red box denotes area shown in Fig. 1c. b) Topography of area shown in Fig. 1a. Vertical error 55m, contour interval 200m. Black box contains 30 fault perpendicular profiles used in generating Figs. 3 and 4. c) Magnified view of portion of Fig. 1a, showing proposed normal fault trace and offsets.

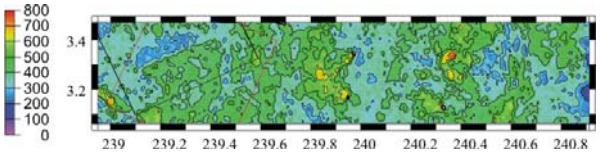

Figure 2. Stereo topography of Manannan area, resolution 80m/pix, vertical error 17m, contour interval 100m. Black box denotes 60 NNW-SSE profiles used in constructing Figs. 3 and 4.

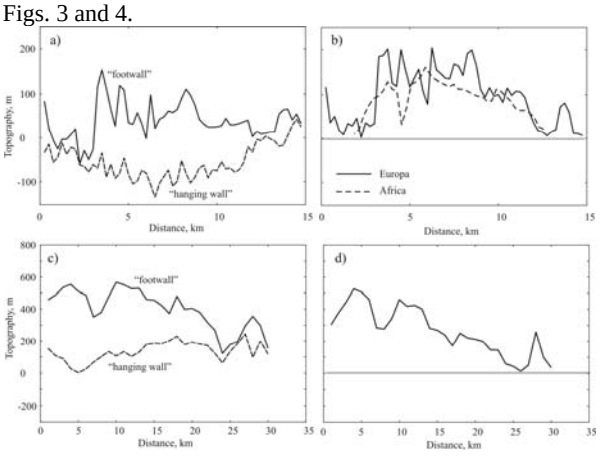

Figure 3 a). Maximum and minimum elevation as a function of distance along fault scarp, from profiles in Fig. 2. b) Vertical displacement across fault, calculated from max/min elevations in a). Dashed line is vertical displacement profile for terrestrial normal fault [13]. c) As for a), but obtained from profiles in Fig. 1b. d) As for b) but using data from c) .

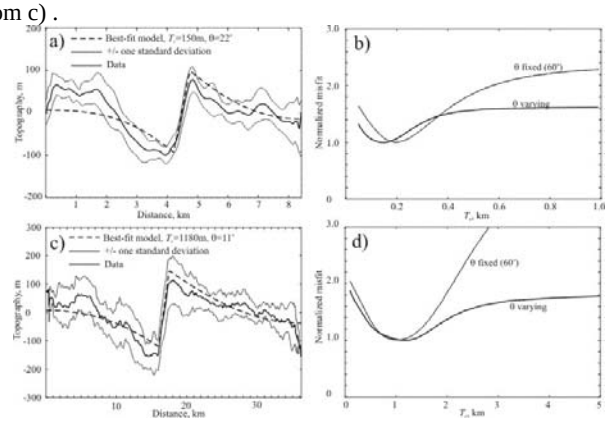

Figure 4 a). Topographic profile across Manannan fault, from central profiles in Fig. 2. Bold line is data, light lines are +/- one standard deviation, dashed line is best-fit model using approach of [5] with T_e=0.15 km. Here we assume a Young's modulus of 1 GPa and a shell thickness of 20 km. b) Normalized misfit as a function of T_e. Bold line allows fault dip to vary, light line keeps fault dip fixed at 60°. c) As for a), but for central profiles from Fig.1b. Best fit T_e is 1.2 km. d) As for b), but for results shown in c).

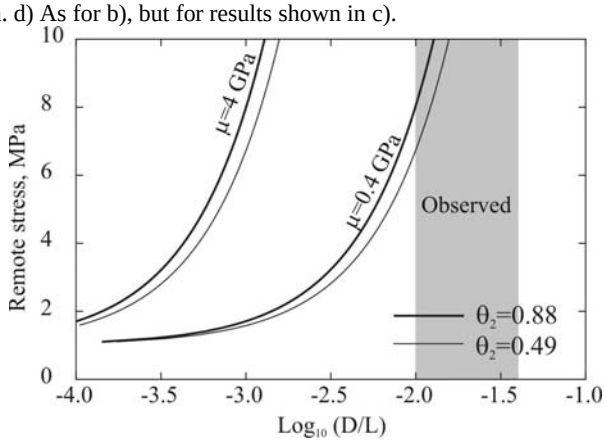

Figure 5. Predicted D/L ratio as a function of remote stress. θ_2 is a constant relating to damage zone width at fault tip (see [6]). Fractured fault strength is 1 MPa, μ is shear modulus. Shaded box denotes the observed D/L ratio.